Supplementary Material (ESI) Journal of Chemical Materials C
This journal is © The Royal Society of Chemistry 2020

Investigations on electron beam irradiated rare-earth doped SrF_2 for application as low fading dosimeter material: Evidence for and DFT simulation of a radiation-induced phase

Michael Arnold[*a], *Julia Katzmann*[b], *Aakash Naik*[c,d], *Arno L. Görne*[a], *Thomas Härtling*[b,e], *Janine George*[c,d], *Christiane Schuster*[b]

[a.] *Fraunhofer Institute for Ceramic Technologies and Systems (IKTS), Michael-Faraday-Strasse 1, 07629 Hermsdorf, Germany*
[b.] *Fraunhofer Institute for Ceramic Technologies and Systems (IKTS), Maria-Reiche-Strasse 2, 01109 Dresden Germany*
[c.] *Bundesanstalt für Materialforschung- und Prüfung, Unter den Eichen 87, 12205 Berlin, Germany*
[d.] *Friedrich-Schiller-University Jena, Institute of Condensed Matter Theory and Solid State Optics, Max-Wien-Platz 1, 07743 Jena, Germany*
[e.] *Institute for Solid State Electronics, Technische Universität Dresden, 01062 Dresden, Germany*

Electronic Supplementary Information (ESI)

Electronic Supplementary Information (ESI) Available: X-ray powder diffraction data for Er- and Yb- doped SrF_2 characterization by the described way of synthesis. Prediction and DFT analyses for the radiation induces phase

Table of Contents

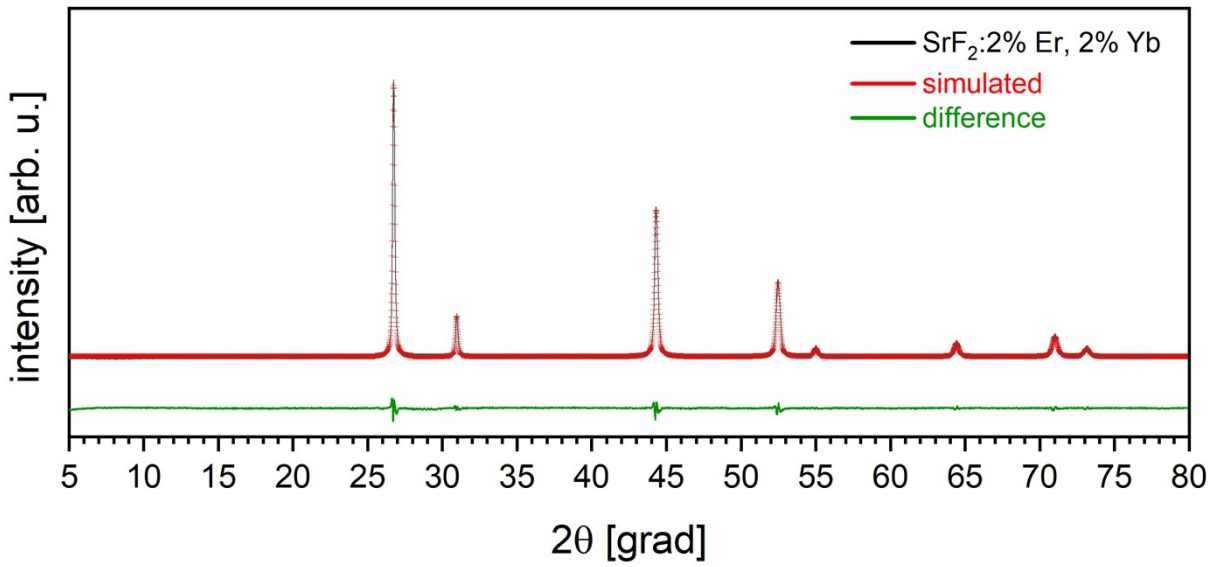

ESI Fig. S1 Comparison of the measured x-ray data (black line) and calculated data (red crosses) for $Sr_{0,94}Er_{0,02}Yb_{0,02}F_2$, RE on Sr-sites, R_p=3.45, R_{wp} = 4.56

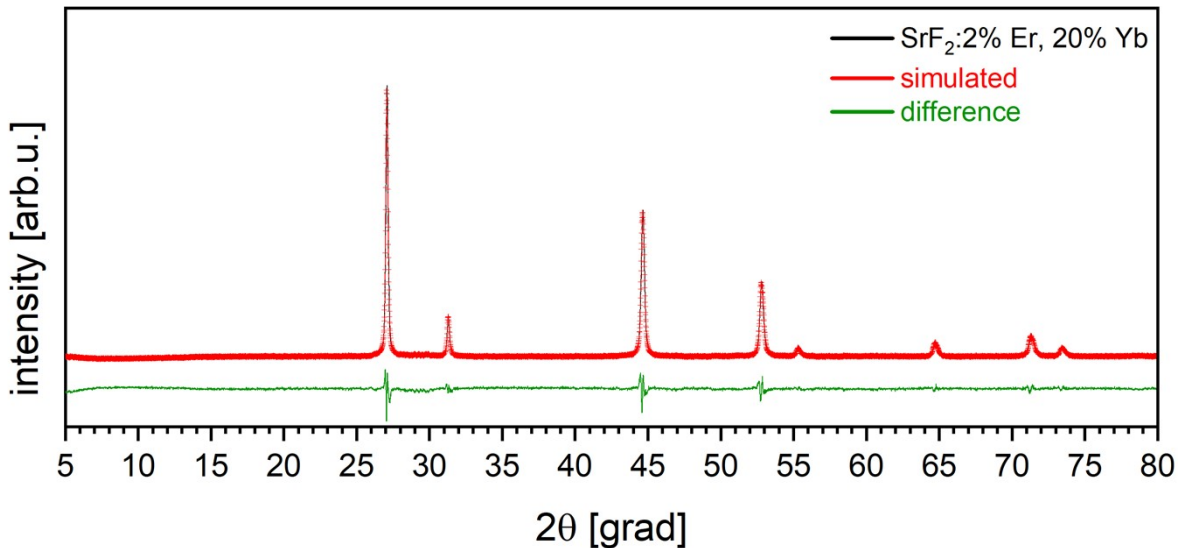

ESI Fig. S2 Comparison of the measured x-ray data (black line) and calculated data (red crosses) for $Sr_{0,78}Er_{0,02}Yb_{0,2}F_2$, RE on Sr-sites, R_p=3.45, R_{wp} = 4.81

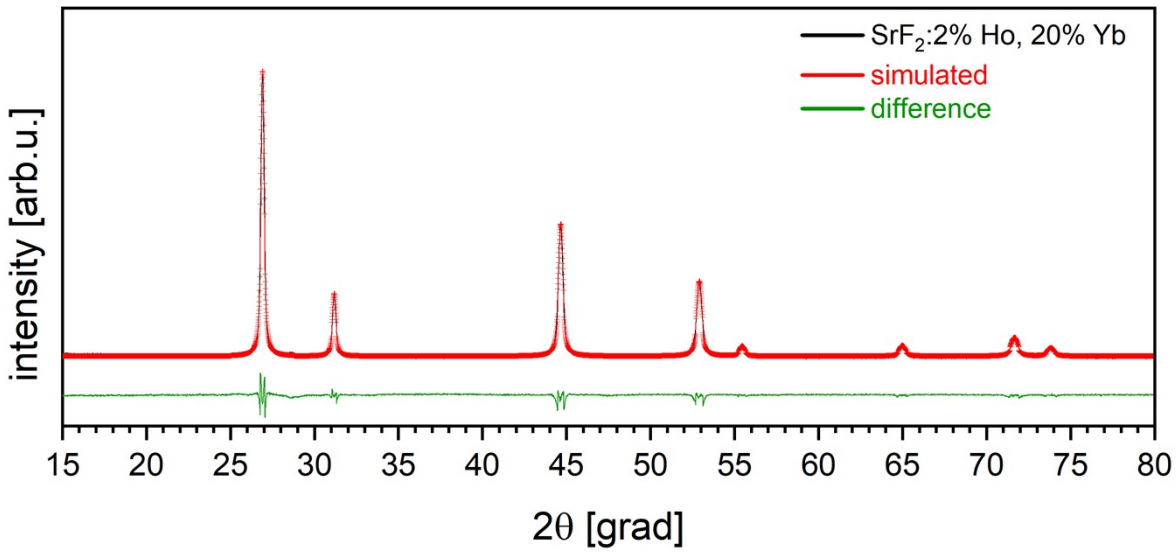

ESI Fig. S3 Comparison of the measured x-ray data (black line) and calculated data (red crosses) for $Sr_{0,78}Ho_{0,02}Yb_{0,2}F_2$, RE on Sr-sites, R_p=5.66, R_{wp} = 7.56

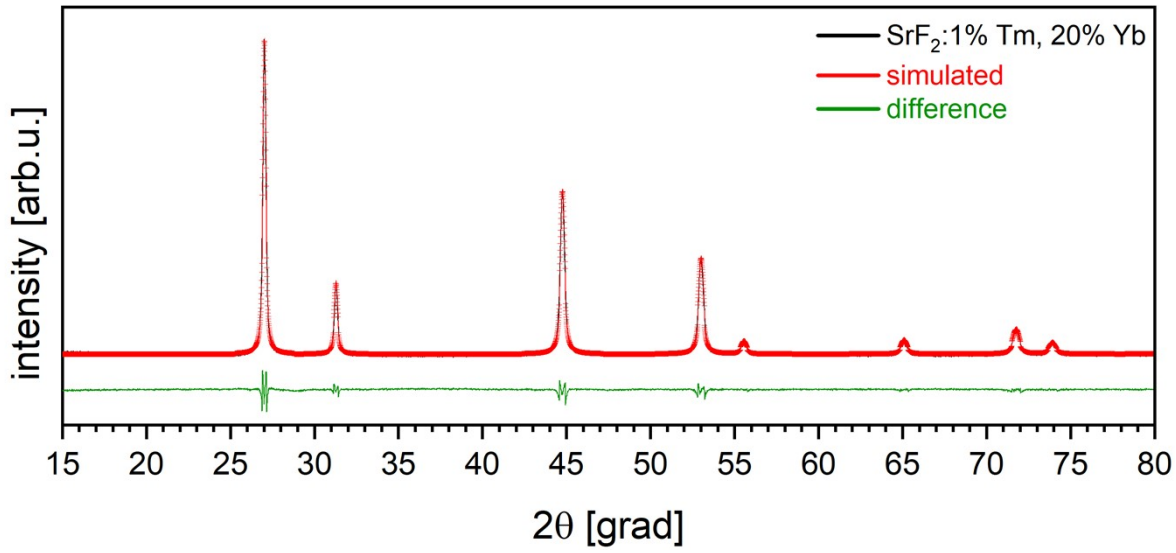

ESI Fig. S4 Comparison of the measured x-ray data (black line) and calculated data (red crosses) for $Sr_{0,79}Tm_{0,01}Yb_{0,2}F_2$, RE on Sr-sites, R_p=3.56, R_{wp} = 5.77

For the refinement of experimental and simulated powder diffraction data using the LeBail algorithm, a decomposition of reflections for an estimation of structure amplitude regarding structure analysis from powder data. It was assumed that the RE dopants replaces the Sr, related to the stochiometric composition in synthesis.

Results for structure prediction with Yb_2OF_2

The predicted structures for Yb_2OF_2 are shown in Figure 5. The corresponding phonon band structures are shown in Figure 5. Total DFT energies and further information on the structures are listed in Table 1 in the main script.

I crystallizes in a P1 space group has 16 different Yb positions. All Yb^{2+} are coordinated by 6 anions. The coordination environments are highly distorted octahedra and trigonal prisms that share. The computed phonon band structure of I shows no imaginary modes.

II is Ilmenite-like structured and crystallizes in the monoclinic Cc space group. There are two inequivalent Yb^{2+} sites. The structure includes a mixture of distorted edge, face and corner-sharing YbO_2F_4 octahedra. The phonon band structure shows small traces of imaginary modes close to the Gamma point. It is slightly less stable than the most stable structure that we found (around 5 kJ/mol per formula unit).

III crystallizes in the orthorhombic Ibam space group. The one inequivalent Yb^{2+} is bonded in a distorted pentagonal planar by two O and 3 F atoms. The structure is derived from a prediction of Sm_2OF_2.

IV is Hazelwoodite-derived structured and crystallizes in the tetragonal $P4_2/mcm$ space group. There is one inequivalent Yb2+. It is bonded in a 6-coordinate geometry to two O and four F atoms. This structure prediction started from the structure of Pb_2OF_2[1]. The phonon band structure and the energetic difference to the most stable structure that we found indicate that this structure is rather unstable (energy difference to the most stable structure >> 35 kJ/mol per formula unit).

V crystallizes in the tetragonal $I4_1/amd$ space group. Yb^{2+} is bonded in a square co-planar geometry by two O and two F atoms. Again, phonon band structure and energetic difference of more than 100 kJ/mol per formula unit to the most stable, predicted structure indicate that this structure is highly unstable. This structure is derived from a prediction of Sm_2OF_2.

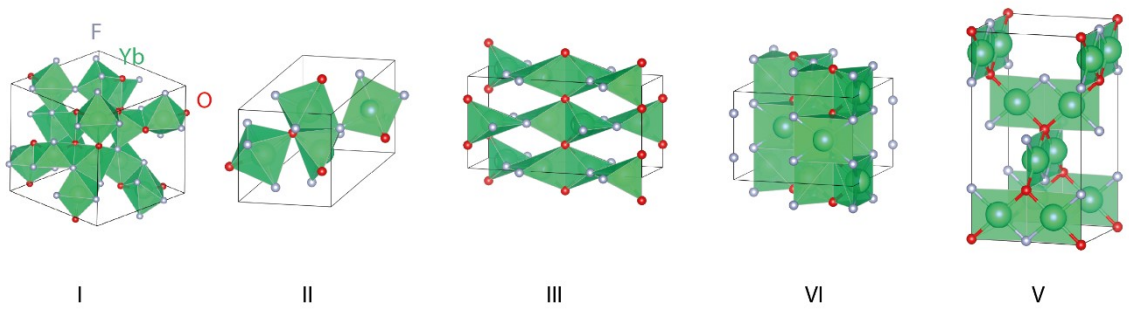

ESI Fig. 5. Predicted structures for Yb_2OF_2.

Methods

We used the structure prediction algorithm[2] and implemented in pymatgen[3] to predict four new structures with the composition Yb2OF2. Originally, the structures of the composition Mn_2OF_2 (mp-761159, mp-759797) and Sn2OF2 (mp-27480, mp-753683) were used. Furthermore, we used a Pb_2OF_2 structure (mp-27355) from the Materials Project[4] and four Sm2OF2 structures (3057555, 3057284, 3091198, 3057286) from the Open Quantum Materials Database[5] as a starting point. We optimized the structures with periodic DFT in VASP[6–9] with strict convergence criteria. After optimization, we arrived at five different structures. We used the PBE functional for all calculations[10]. All k-point settings were converged and can be found in the raw data. For electronic and structural optimization, a criterion of $\Delta E < 10\text{-}7$ and $\Delta E < 10\text{-}5$ eV per cell was used, respectively. Once the optimized structures were obtained, the harmonic interatomic force constants were computed using the finite displacement method as implemented in Phonopy[11], with a displacement of 0.01 Å and with the help of supercell of the optimized cell (with cell parameters as close as possible to 20 Å or larger in each direction). The forces for this evaluation were computed at the Γ-point. Using a larger super cell is not feasible. The raw data can be downloaded here: link

The depicted band structures have not been corrected with the non-analytical term correction around the Gamma point. The robocrystallographer[12] and ChemEnv[13] were used to help with describing the newly predicted structures. VESTA[14] was used for visualization.

The Open Quantum Materials Database (OQMD) is a high-throughput database currently consisting of nearly 300.000 density functional theory (DFT) total energy calculations of compounds from the Inorganic Crystal Structure Database (ICSD) and decorations of commonly occurring crystal structures.

Based on chemical similarity (similarities of ionic radii of Yb^{2+} with other ions) and predicted structures, we selected one structure from the OQMD database as a starting point. We identified the structure type Pd_2OF_2 [15], which in the OQMD is forecasted for Sm_2OF_2 as a Pd_2OCL_2 like structure. We proceed to refine this structural model. We start with the structural parameters of this compound with the space group I41/amd (141). The symmetry can be easily converted into the group $P4_2nnm$ (137) with the half lattice parameter c. The intensity ratio of the most intensive reflexes (111) and (-311) and the other reflexes are an almost coincidence of observed powder pattern. For stoichiometry, fluorine occupies Wycoff positions 4c, Oxygen the position 2a and Ytterbium 4f. By replacing Sm with Yb and a short refinement of the lattice parameters (a = 5,2199 Å, b = 5.2264 Å), the calculated reflexes get coincident with the observed ones (Figure 8, blue line). There are, however, some smaller reflexes that are not explained with this structural model. To confirm and understand our structural model further, we turned to DFT-based harmonic phonon computations and performed our own DFT-based structural predictions. Computed phonon band structures allow to confirm the dynamical stability of a compound and can give information on the plausibility of a structural model. Further computational details can be found in the method section of this publication.
Unfortunately, the structural model based on Sm_2OF_2 showed servere dynamical instabilities in the DFT-based phonon band structure after structural optimization which typically are connected to phase transitions of a compound. To arrive at a potentially more stable structural model, we used DFT-based structure prediction based on plausible element substitutions that have been determined based on data mining. [21] This structure prediction algorithm is implemented in pymatgen[3]. We used it to predict additional structures with the composition Yb_2OF_2 and compared them to the model based on the hypothetical Sm_2OF_2 structure. Originally, these structural models stem from the Materials Project Database and the corresponding identifiers from the Materials Project database are listed in Table 2.
The dynamically stable structure is also the structure with the lowest total DFT energy (Table 1. This structure is based on a predicted Mn_2OF_2 structure from the Materials Project. Figure 6 shows the phonon band structure of this structural model. VESTA[27] was used for visualization (Figure 7).

ESI Tab. 1: The five structures as the starting point for the DFT calculation. Yb2OF2 with space group no. 1 (1st row) turned out to be the dynamically and energetically most stable structure.

Compound	Space group	OQMD / Materials project (mp)	Relative energy per formula unit
Mn2OF2	P1 (1)	mp-761159	0
Mn2OF2	Cc (9)	mp-759797	4.55
Sm2OF2	Ibam (72)	3057555	29.65
Pb2OF2	P42nnm (137)	mp-27355	36.81
Sm2OF2	I41/amd (141)	3057286	109.65

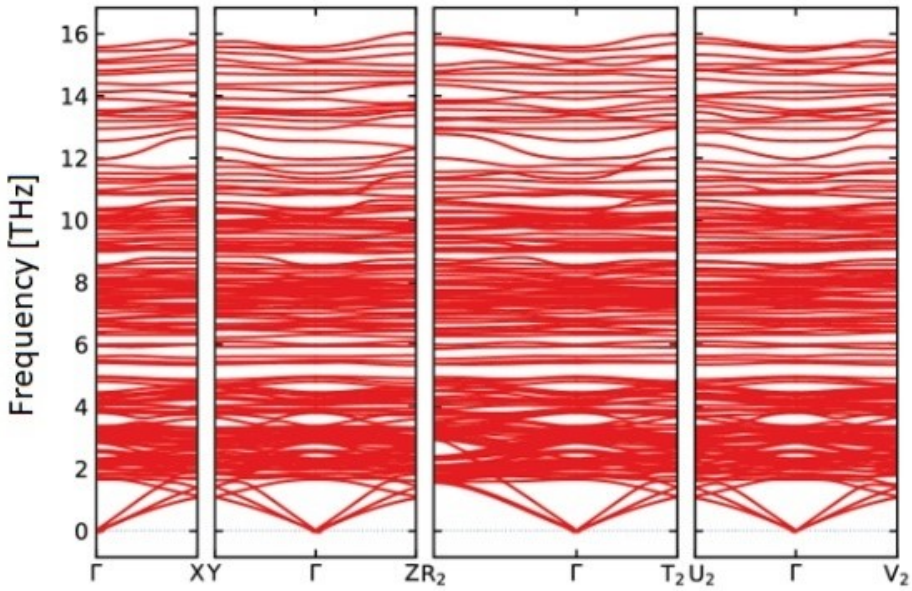

ESI Fig. S6: Phonon band structures for the Yb_2OF_2 compounds that are shown in Figure 5 (I).

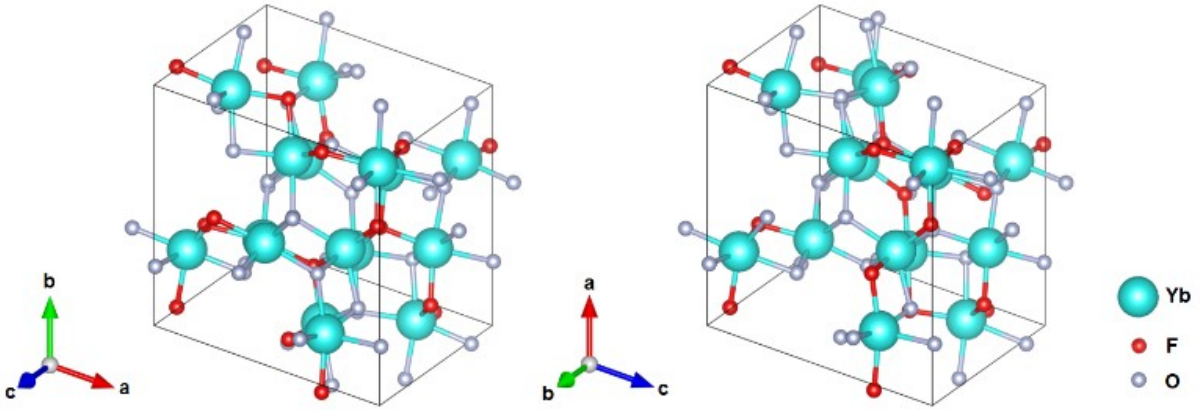

ESI Fig. S7: Most stable predicted structure for Yb_2OF_2 by the DFT calculations as visualized by VESTA.

Short description of elementary Cell

DFT predicts lattice constants of a = 9.17429 Å, b = 9.16096 Å and c = 9.21875 Å and angles of a = 109.4281 °, b = 109.4893 ° and g = 109.2381 °. The simulated powder diffractogram on the base of our DFT calculation is shown in Figure 7 (red line). The reflexes almost coincide with the observed powder pattern (Figure 8 in the main paper). A short refinement of the lattice constants and angles is necessary. The data after the refinement are a = 9.05630 Å, b = 9.04980 Å and c = 9.04250 Å and the angles at a = 109.4950 °, b = 109.4850 ° and g = 109.4560 °. A decrease of the cell volume from 598.3260 $Å^3$ to 570.343557 $Å^3$ is observed. It is well-known that typical GGA functionals such as PBE overestimate the experimental lattice parameters[14]. The unit cell has 16 different Yb positions and 8 oxygen and 16 fluorine coordinates. All Yb^{2+} are coordinated by 6 anions (F and O). The structure predicted from DFT, therefore, seems to agree with the experimental results. Because the harmonic phonons are free from imaginary modes, we have additional confidence in this structural prediction.

Dosimetric standards

To support the dosimetric properties of doped SrF_2 phosphors, we compare the dose response with established the established materials B3, a radiochromic film dosimeter, and alanine, a reference dosimeter material (with dose responses for B3 graphically extracted from Ref. [16] and for alanine from https://www.harwell-dosimeters.co.uk/wp-content/uploads/2014/05/alanine-curve.png). Since the physical properties read out (luminescent decay time versus absorbance for B3, electron paramagnetic resonance for alanine), and thus absolute numerical values, are different, only normalized dose responses can be compared. Note that the dose response of our phosphors is calculated as $1/\tau–1/\tau_0$ (with τ the luminescence decay time, and τ_0 the luminescence decay time in the unirradiated state): the phosphors, unlike B3 and alanine, show a decrease in decay time with increasing dose. As shown in the figure below, the dose response, and thus the dose sensitivity, of both classes of materials are very comparable.

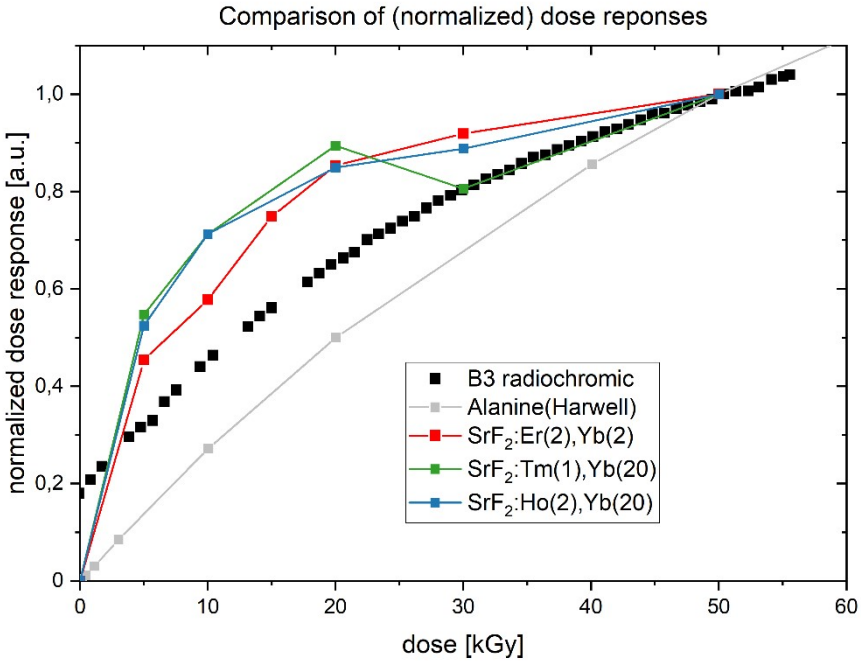

ESI Fig. S8: Comparison of the normalized dose response of different co-dopings of SrF_2 to the dosimetric standard materials B3 and Alanine

Refences

1 B. Aurivillius, *Chemica Scripta*, 1976, **10**, 156–158.
2 G. Hautier, C. Fischer, V. Ehrlacher, A. Jain, G. Ceder, *Inorg. Chem.,* 2011, **50**, 656–663.
3 S. P. Ong, W. D. Richards, A. Jain, G. Hautier, M. Kocher, S. Cholia, D. Gunter, V. L. Chevrier, K. A. Persson, G. Ceder, *Comput. Mater. Sci.*, 2013, **68**, 314.
4 A. Jain, S. P. Ong, G. Hautier, W. Chen, W. D. Richards, S. Dacek, S. Cholia, D. Gunter, D. Skinner, G. Ceder, K. A. Persson, *APL Mater.*, 2013, **1**, 011002.
5 S. Kirklin, J. E. Saal, B. Meredig, A. Thompson, J. W. Doak, M. Aykol, S. Rühl, C. S. Wolverton, *Comput. Mater.,* 2015, **1**, 15010.
6 G. Kresse, J. Hafner, *Phys. Rev. B*, 1993, **47**, 558.
7 G. Kresse, J. Hafner, *Phys. Rev. B*, 1994, **49**, 14251.
8 G. Kresse, J. Furthmüller, *Phys. Rev. B*, 1996, **54**, 11169.
9 G. Kresse, J. Furthmüller, *Comput. Mater. Sci.,* 1996, **6**, 15–50.
10 J. P. Perdew, K. Burke, M. Ernzerhof, *Phys. Rev. Lett.*, 1996, **77**, 3865–3868.
11 A. Togo, I. Tanaka, *Scr. Mater*. 2015, **108**, 1.

12 A. M. Ganose, A. Jain, *MRS Commun*., 2019, **9**, 874–881.
13 D. Waroquiers, J. George, M. Horton, S. Schenk, K. A. Persson, G.-M. Rignanese, X. Gonze, G. Hautier, *Acta Cryst B*, 2020, **76**, 683–695.
14 K. Momma, F. Izumi*, J. Appl. Crystallogr*., 2011, **44**, 1272–127
15 R. Dronskowski, Computational Chemistry of Solid State Materials, A Guide for Materials Scientists, Chemists, Physicists and Others, Wiley-VCH, Weinheim, 2005.
16 J. Helt-Hansen, A. Miller, M. McEwen, P. Sharpe, S. Duane, *Radiat. Phys. Chem.,* 2004, **71**, 355–359.